

# Indirect Power Control of a Variable Speed Wind Turbine Based on Doubly Fed Induction Generator

**Aziz Boukadoum<sup>1\*</sup>, Abla Bouguerne<sup>1</sup>, Mohamed Salah Djebbar<sup>1</sup>,  
Atef Ahriz<sup>2</sup>, Tahar Bahi<sup>3</sup>**

<sup>1</sup> Labget Laboratory, Department of Electrical Engineering, Echahid Cheikh Larbi Tebessi University, Algeria

<sup>2</sup>LGCA laboratory, Department of Architecture, Echahid Cheikh Larbi Tebessi University, Algeria

<sup>3</sup>Laza laboratory, Department of Electrical Engineering, University of Annaba, Algeria

\*Corresponding Author: [aziz.boukadoum@univ-tebessa.dz](mailto:aziz.boukadoum@univ-tebessa.dz)

## Abstract

*In this work, performances static and dynamic improvement of wind energy conversion system connected to the grid is presented. The system is based on a double-fed induction generator (DFIG) connected to the variable wind speed. After analyzing the mechanical part of the wind turbine and seeing the simplified mathematical model of the DFIG, a vector control is necessary to decouple the active and reactive powers in order to properly control the stator powers to allow proper operation of the wind turbine. In this paper, we present a simulation study of an indirect power control algorithm of wind conversion system connected to the grid, using PI controller via maximum power point tracking (MPPT) strategy. The performance of the system control was analyzed and compared in terms of robustness under parameter variation.*

**Keywords:** Wind Turbine, IDPC, DFIG, PI controller, Performances improvement.

### 1 Introduction

Following the strong growth in electricity consumption, energy will always remain an energy that humanity will no longer be able to do without. Fossil fuels have long been used in the production of electrical energy; these fossil fuels cause harmful damage to the environment [1]. To meet the high demand for energy while preserving the environment, the majority of countries have opted for the use of renewable energies. These energies are inexhaustible, clean and do not create greenhouse gases unlike fossil fuels [2, 3]. Wind energy is the fastest growing renewable energy in the world. It is almost universally recognized as the most promising energy source for producing clean electricity in the short to medium term. In addition, it contributes to the preservation of the environment [4]. However, the problem is that this resource is characterized by a variable wind speed [5]. For this reason, we have opted for a double fed induction generator (DFIG), this machine makes it possible to extract maximum power from a given wind speed by optimizing the specific speed, and minimizing the mechanical stresses on the turbine during gusts of wind. As well as other benefits such as; reduce the dimensioning of converters and improve the quality of the energy produced. On the other hand, the control of this machine remains the most important and the most complex phase [6]. Thus, we will begin our study with the modeling of the wind turbine then, the modeling of the DFIG, and the power control, which is done by vector control. Finally, the results of the simulations will be presented in the Matlab/simulink in order to deduce the effectiveness of control system. See Figure 1.

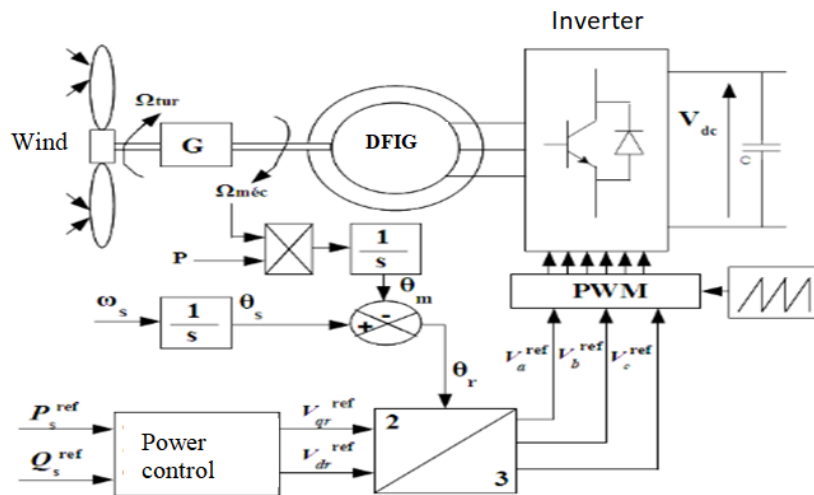


Figure 1 Structure of wind power conversion system.

### 2 Method and materials

#### 2.1 Wind turbine modeling

The wind turbine allows the transformation of kinetic energy into mechanical energy and then into electrical energy through a generator. Wind power depends on the surface to be swept (S), wind speed (v) and air density (ρ). Based on the fluid mechanics equations we have the following equation [7-9].

The aerodynamic power  $P_{tur}$  captured by the wind turbine is given by:

$$P_{tur} = \frac{1}{2} C_p(\lambda, \beta) \cdot \rho \cdot S \cdot v^3 \tag{1}$$

Where:

$\rho$  : is the air density (1.22 kg/m<sup>3</sup>) ;

$S$ : is wind turbine blades swept area in the wind (m<sup>2</sup>)

$R$  : is the turbine radius (m) ;

$v$  : is wind speed(m/s) ;

$\beta$  : blade pitch angle (°)

$\lambda$  : is the tip-speed ratio defined by:

$$\lambda = \frac{\Omega_{tur} \cdot R}{v} \quad (2)$$

$C_p$ : is the power coefficient of wind is treated in bibliographies for a wind of 1.5MW by:

$$C_p(\lambda, \beta) = 0.5 \left[ \left( \frac{116}{\lambda_i} - 0.4\beta - 5 \right) e^{\frac{-21}{\lambda_i}} + 0.0068\lambda \right] \quad (3)$$

With:

$$\frac{1}{\lambda_i} = \frac{1}{\lambda + 0.08\beta} - \frac{0.035}{\beta^3 + 1} \quad (4)$$

Expression of the aerodynamic torque is given by [10, 11]:

$$T_{tur} = \frac{P_{tur}}{\Omega_{tur}} = \frac{\pi}{2\lambda} \rho \cdot R^3 \cdot C_p(\lambda, \beta) \quad (5)$$

The multiplier is the connection between the turbine and the generator modeled by [12, 13]:

$$T_{mec} = \frac{T_{tur}}{G} \quad (6)$$

$$\Omega_{mec} = G \cdot \Omega_{tur} \quad (7)$$

Where:

$T_{mec}$  : is mechanical torque,

$\Omega_{tur}, \Omega_{mec}$  : are the turbine and generator speed, and

$G$  is the multiplier ratio.

The equation of system dynamics can be written as :

$$J \frac{d\Omega_{mec}}{dt} + f \cdot \Omega_{mec} = T_{mec} - T_{em} \quad (8)$$

Where:

$f$  : is the viscous friction coefficient,

$T_{em}$  : is the electromagnetic torque of the generator.

Figure 2 present schema bloc of wind turbine without speed control

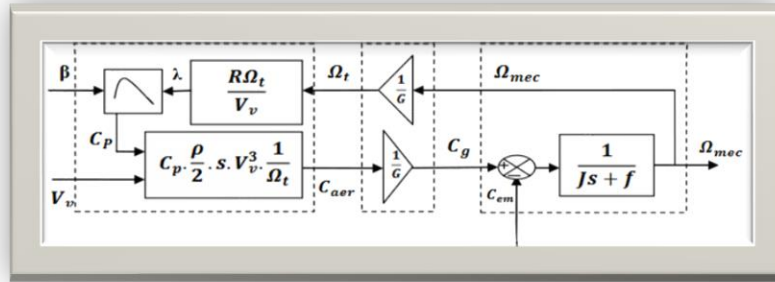


Figure 2 Bloc diagram of wind turbine

### 2.2 Modeling of DFIG

The DFIG model is no more different than the model of the induction machine with squirrel cage but the DFIG is not short-circuited. To control a dynamic system, the stator of the machine is directly connected to the power grid, but the rotor is connected through the power electronics. The mathematical model of DFIG in the park referential (d-q) is given by the following equations [14, 15], see figure 3:

The electrical equations of the stator and rotor voltages of the DFIG are written:

$$\begin{cases} V_{sd} = R_s \cdot I_{sd} + \frac{d}{dt} \Phi_{sd} - \omega_s \cdot \Phi_{sq} \\ V_{sq} = R_s \cdot I_{sq} + \frac{d}{dt} \Phi_{sq} + \omega_s \cdot \Phi_{sd} \\ V_{rd} = R_r \cdot I_{rd} + \frac{d}{dt} \Phi_{rd} - \omega_r \cdot \Phi_{rq} \\ V_{rq} = R_r \cdot I_{rq} + \frac{d}{dt} \Phi_{rq} + \omega_r \cdot \Phi_{rd} \end{cases} \quad (9)$$

The stator and rotor flux are expressed by:

$$\begin{cases} \Phi_{sd} = L_s \cdot I_{sd} + M \cdot I_{rd} \\ \Phi_{sq} = L_s \cdot I_{sq} + M \cdot I_{rq} \\ \Phi_{rd} = L_r \cdot I_{rd} + M \cdot I_{sd} \\ \Phi_{rq} = L_r \cdot I_{rq} + M \cdot I_{sq} \end{cases} \quad (10)$$

Where:

$R_s, R_r, L_s$  and  $L_r$  : are respectively the resistance and inductance of the stator and the rotor;

$M$  : is the mutual inductance,

$I_{sd}, I_{sq}, I_{rd}, I_{rq}$  represent the d and q components of the stator and rotor currents;

$\omega_s$  is the stator angular frequency ( $\omega_r = \omega_s - p\Omega_{mec}$ )  $\omega_r$  is rotor angular frequency and  $p$  is number of pole pairs.

Equation (11) represents the expression of electromagnetic torque:

$$T_{em} = p \frac{M}{L_s} (\Phi_{sd} I_{rd} - \Phi_{sq} I_{rd}) \quad (11)$$

The active and reactive powers in the stator and rotor of the DFIG are given respectively:

$$\begin{cases} P_s = (V_{sd} \cdot I_{sd} + V_{sq} \cdot I_{sq}) \\ Q_s = (V_{sq} \cdot I_{sd} + V_{sd} \cdot I_{sq}) \\ P_r = (V_{rd} \cdot I_{rd} + V_{rq} \cdot I_{rq}) \\ Q_s = (V_{rq} \cdot I_{rd} - V_{rd} \cdot I_{rq}) \end{cases} \quad (12)$$

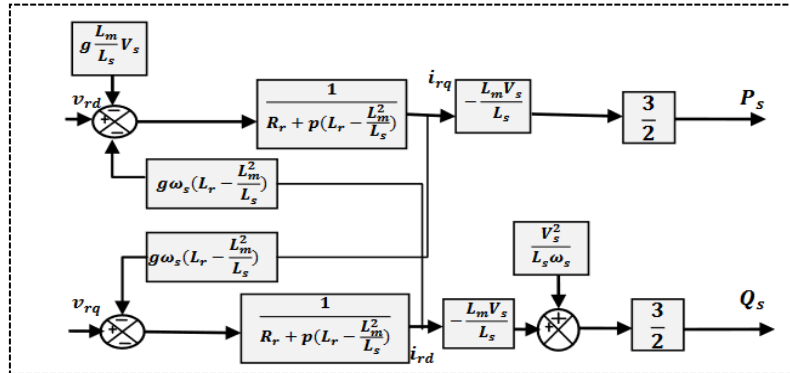


Figure 3 Block diagram of DFIG

### 2.3 Field oriented control

The principle of vector control is to orient the flux of the machine in one of the two axes d or q. In our case and in order to simplify the control of stator power (active or reactive), we use an orientation on the d axis [16-20]. However:  $\Phi_{sq} = 0$  and  $\Phi_{sd} = \Phi_s$

The expressions of the electromagnetic torque become:

$$T_{em} = -\frac{3}{2} p \cdot \frac{M}{L_s} \cdot \Phi_{sd} \cdot I_{rq} \quad (13)$$

The expression of the stator voltages becomes:

$$\begin{cases} V_{sd} = R_s \cdot I_{sd} + \frac{d}{dt} \Phi_{sd} \\ V_{sq} = R_s \cdot I_{sq} + \omega_s \cdot \Phi_{sd} \end{cases} \quad (14)$$

For medium and high power machines, stator resistances are neglected, therefore the stator voltage equations become:

$$\begin{cases} V_{sd} = \frac{d}{dt} \Phi_{sd} \\ V_{sq} = \omega_s \cdot \Phi_{sd} \end{cases} \quad (15)$$

In steady state, it is assumed that the flow is constant, thus:

$$\begin{cases} V_{sd} = 0 \\ V_{sq} = \omega_s \cdot \Phi_{sd} = V_s \end{cases} \quad (16)$$

$$\begin{cases} \Phi_{sd} = \Phi_s = L_s \cdot I_{sd} + M \cdot I_{rd} \\ \Phi_{sq} = 0 = L_s \cdot I_{sq} + M \cdot I_{rq} \end{cases} \quad (17)$$

From the (17), we deduce the equations linking between stator and rotor currents:

$$\begin{cases} I_{sd} = \frac{\Phi_s}{L_s} - \frac{M}{L_s} \cdot I_{rd} \\ I_{sq} = -\frac{M}{L_s} \cdot I_{rq} \end{cases} \quad (18)$$

The relations of the powers become:

$$\begin{cases} P_s = V_{sq} \cdot I_{sq} \\ Q_s = V_{sq} \cdot I_{sd} \end{cases} \quad (19)$$

To express the power relations as a function of the rotor currents, we replace in the previous equation the currents by the (20):

$$\begin{cases} P_s = -V_s \cdot \frac{M}{L_s} I_{rq} \\ Q_s = \frac{V_s}{L_s} \Phi_s - V_s \cdot \frac{M}{L_s} \cdot I_{rq} = \frac{V_s^2}{L_s \cdot \omega_s} - V_s \cdot \frac{M}{L_s} \cdot I_{rq} \end{cases} \quad (20)$$

By replacing flux and stator currents in the (10) by the expression (18) we obtain:

$$\begin{cases} \Phi_{rd} = (L_r - \frac{M^2}{L_s}) \cdot I_{rd} + M \frac{V_s}{L_s \cdot \omega_s} \\ \Phi_{rq} = (L_r - \frac{M^2}{L_s}) I_{rq} \end{cases} \quad (21)$$

In order to control the generator, these expressions are established showing the relationship between the currents and the rotor voltages that will be applied to it.

$$\begin{cases} V_{rd} = R_r \cdot I_{rd} + L_r \sigma \frac{dI_{rd}}{dt} - g \omega_s L_r \sigma I_{rq} \\ V_{rq} = R_r \cdot I_{rq} + L_r \sigma \frac{dI_{rq}}{dt} - g \omega_s L_r \sigma I_{rd} + g \cdot \frac{V_s M}{L_s} \end{cases} \quad (22)$$

Where:

$$\sigma = (1 - \frac{M^2}{L_s L_r}) \text{ is the dispersion coefficient.}$$

We have two methods of Field Orientation Control [20-21].

### 2.3.1 Direct power control

This control method was proposed by Blaschke [22]. In this case, the idea on the regulation consists in independently and directly controlling the powers  $P_s$  and  $Q_s$  of the DFIG, in which the decoupling terms will be neglected. The diagram in figure 4 presents the principle of so-called direct control. If we notice the equation (22), we see that the rotor currents are linked to the active and reactive powers by the term  $\frac{L_m V_s}{L_s}$ . Similarly, the terms involving the derivatives of the two-phase rotor currents in the system (22) disappear in steady state. So we have :

$$\begin{cases} V_{dr} = R_r I_{dr} - g \omega_s \left( L_r - \frac{L_m^2}{L_s} \right) I_{qr} \\ V_{qr} = R_r I_{qr} - g \omega_s \left( L_r - \frac{L_m^2}{L_s} \right) I_{dr} + g \frac{L_m V_s}{L_s} \end{cases} \quad (23)$$

$V_{dr}$  and  $V_{qr}$  are the two-phase components of the rotor voltages to be imposed on the machine to obtain the desired rotor currents.

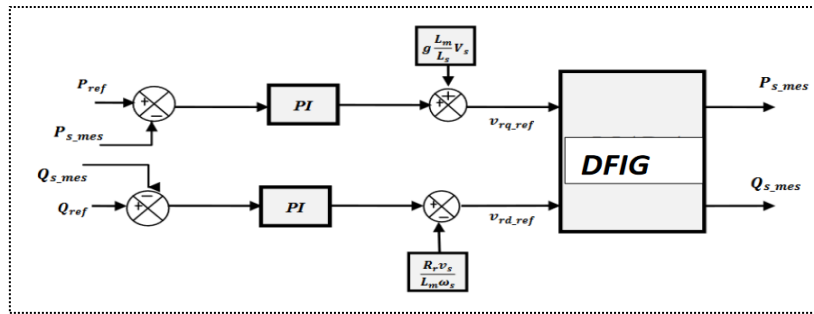


Figure 4 Direct control block diagram

The effect of the coupling term  $g\omega_s \left( L_r - \frac{L_m^2}{L_s} \right)$  is minimal for low slips and can be compensated by an adequate synthesis of the regulators in the control loop. On the other hand, the term  $g \frac{L_m V_s}{L_s}$  represents an electromotive force whose influence is not negligible. The control system will therefore have to compensate for this disturbance. Thus, we obtain a simpler model allowing the direct and independent control of the active and reactive powers by using a single regulator on each axis [23-25].

**2.3.2 Indirect power control**

This method consists in summarizing the control operation from the inversion of the transfer function of the system to be regulated, to establish the reference rotor voltages as a function of the active and reactive powers at the level of the stator [26-30].

**2.3.2.1 Open loop control**

Open loop control is essentially based on the assumption of a stable network in voltage and frequency, it consists of slaving not the powers but rather indirectly the rotor currents by no longer using the powers measured as a return on the comparator but the rotor currents of axis d and q [31]. From the equations of the stator active and reactive power of the system, we can conclude the references of the direct and quadrature rotor currents according to the relationships:

$$\begin{cases} I_{qr-ref} = -\frac{2L_s}{3L_m V_s} P_{sref} \\ I_{dr-ref} = -\frac{2L_s}{3L_m V_s} Q_{sref} + \frac{V_s}{\omega_s L_m} \end{cases} \quad (24)$$

These currents will be used as references instead of the active and reactive power references, as shown in figure 5. This development remains reliable as long as the electrical network remains stable in voltage and frequency. Network instability will therefore create an error in the monitoring of the active and reactive power set points.

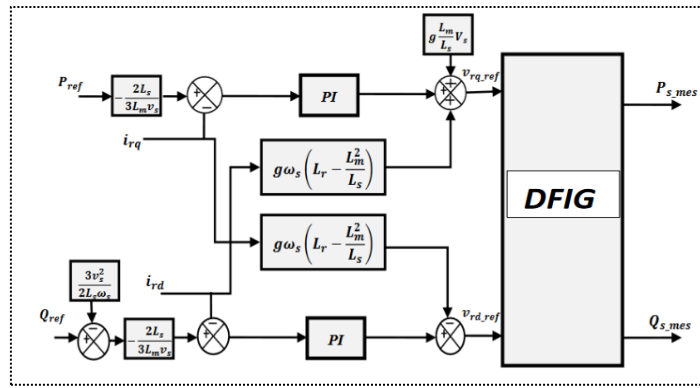


Figure 5 Block diagram of indirect control in open loop.

This method consists in summarizing the control operation from the inversion of the transfer function of the system to be regulated, to establish the reference rotor voltages as a function of the active and reactive powers at the level of the stator. It is therefore sought to form the equations of the active and reactive powers on the one hand and of the rotor voltages on the other hand according to the rotor currents while taking into account the mathematical model of the generator.

**2.3.2.2 Closed loop control**

To regulate the powers in an optimal way, we are going to set up two regulation loops on each axis with a proportional integral regulator for each, one loop on the power and the other on the corresponding current while compensating for the terms of disturbances and couplings appearing on the block diagram of the MADA model. We thus obtain the command structure shown in figure 6 [32-33]:

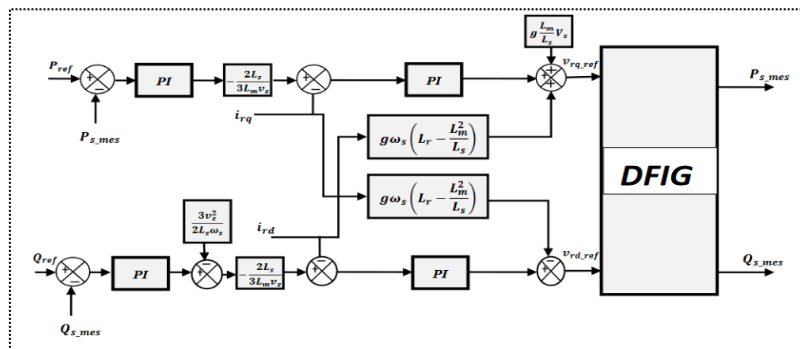


Figure 6 Block diagram of closed loop indirect control

**2.3.2.3 PI controller**

The use of PI controller is simple and quick to implement while offering acceptable performance. Figure 7 shows part of the looped system corrected by a PI controller [34-38].

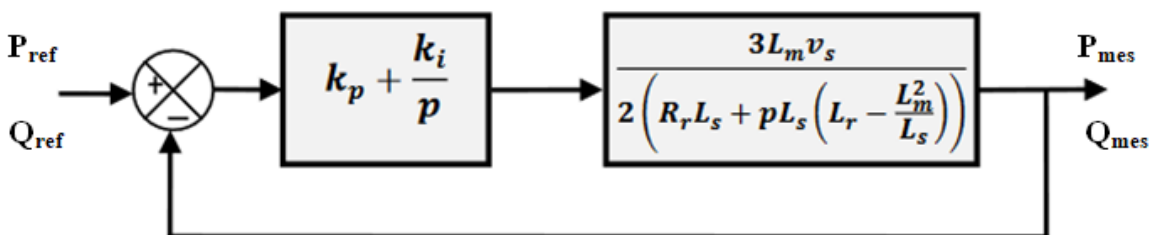


Figure 7 Schema bloc PI controller

In this perspective, the open loop transfer function integrating the presence of regulators is [25]:

$$FTBO = \frac{P + \frac{k_i}{k_p}}{\frac{P}{k_p}} \cdot \frac{\frac{3L_m V_s}{2\sigma L_r L_s}}{P + \frac{R_r L_s}{\sigma L_r L_s}} \quad (25)$$

$$\text{With: } \sigma = 1 - \frac{L_m^2}{L_s L_r}$$

To eliminate the zero present in the transfer function, we select the pole compensation formula for the regulator synthesis, which results in the following equality:

$$\frac{k_i}{k_p} = \frac{R_r L_s}{\sigma L_r L_s} \quad (26)$$

It will be noted here that the advantage of pole compensation is only apparent if the parameters of the generator are determined with precision because the gains  $k_p$  and  $k_i$  are established as a function of these same parameters. If the actual parameters are different from those used in the synthesis, the compensation is ineffective. If the poles are perfectly compensated, the open loop transfer function becomes:

$$FTBO = \frac{K_p \frac{3L_m V_s}{2\sigma L_r L_s}}{P} \quad (27)$$

The closed loop transfer function is then expressed by:

$$FTBF = \frac{1}{1 + P\tau_r} \quad (28)$$

With;

$$\tau_r = \frac{1}{k_p} \frac{2\sigma L_r L_s}{3L_m V_s}$$

The term  $\tau_r$  here shows the time constant of the system. From now on, we can express the gains of the correctors according to the parameters of the generator and the response time:

$$k_p = \frac{1}{\tau_r} \frac{2\sigma L_r L_s}{3L_m V_s} \quad (29)$$

$$k_i = \frac{1}{\tau_r} \frac{2L_r L_s}{3L_m V_s} \quad (30)$$

The energy conversion chain adopted for the MADA power supply consists of a single rotor converter composed of a diode rectifier and an inverter, which are connected to each other via a low pass filter. On the other hand, the stator is connected directly to the three-phase source. For inverter control, the triangular-sinusoidal PWM technique is used [25].

#### 2.3.2.4 Model of inverter

the structure of the three-phase two-level inverter is shown in Figure 8.

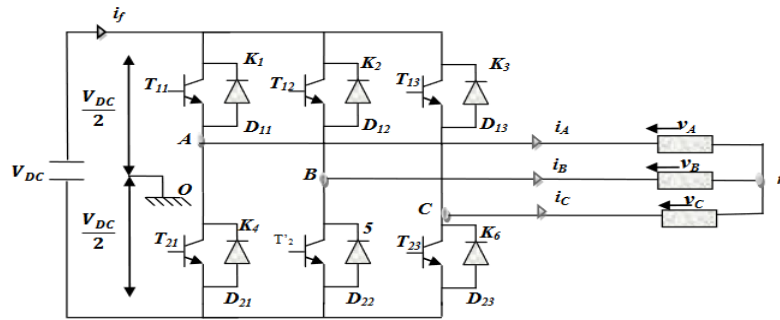


Figure 8 Structure of three phase inverter.

Each transistor/diode assembly corresponds to an ideal switch. The state of each switch is quantified by a connection function ( $S_{ij}$ ) we define this function of switching as follows:

$$S_{ij} = \begin{cases} 1 & \text{if } S_{ij} \text{ is closed} \\ 0 & \text{if } S_{ij} \text{ is open} \end{cases}$$

Using the principle of the ( $F_{ij}$ ) connection function of the ( $S_{ij}$ ) switches, the output voltages of the inverter are expressed according to the following equations:

$$\begin{cases} V_a = \frac{1}{3}(2F_{11} - F_{21} - F_{31}) \cdot V_{dc} \\ V_b = \frac{1}{3}(-F_{11} + 2F_{21} - F_{31}) \cdot V_{dc} \\ V_c = \frac{1}{3}(-F_{11} - F_{21} + 2F_{31}) \cdot V_{dc} \end{cases} \quad (31)$$

The voltage across the DC bus capacitor is given by the following relationship:

$$\frac{dV_{dc}}{dt} = \frac{1}{C} I_c \quad (32)$$

$I_c$ : is the current in the capacitor

The control algorithm of the switches of the first arm of the inverter is illustrated in Figure 9, In SPWM technique three sine waves and a high frequency triangular carrier wave are used to generate PWM signal

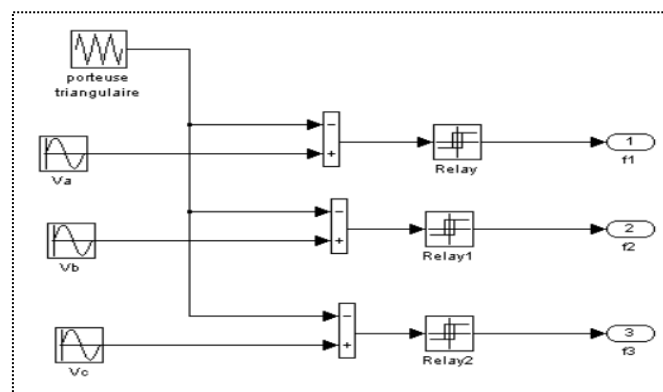


Figure 9 Generation of inverter PWM control signals

### 3. Results and discussion

The simulation allowed us to check the reliability of the control. We have chosen a wind profile which will be applied for the wind turbine. This profile is characterized by a relatively low value around (10 m/s). The simulation results show that the variation of the electrical power is

adapted to the variation of the speed of the generator, and the latter is adapted to the variation of the wind speed. This shows the influence of variations in wind speed on the mechanical speed and subsequently on the electrical power produced. The parameters of proposed conversion system are shown in Table 1.

Table 1 System parameters

Parameters, units	Values
<b>DFIG</b>	
Grid frequency $f_s$	50 Hz
Grid voltage $V_{srms}$ ,	220V
Voltage $V_{rrms}$ ,	220V
Power $P_n$	0.5MW
Voltage (line-line) $U_{nrms}$ ,	380V
Stator resistance $R_s$	0.0063 $\Omega$
Stator Inductance $L_s$	0.018 H
Rotor resistance $R_r$ , $\Omega$	0.0048 $\Omega$
Rotor Inductance $L_r$	0.0116H
Mutual inductance $L_m$	0.0115H
Inertia $J$	50Kg.m <sup>2</sup>
number of pole pairs	2
<b>PI Controller</b>	
Kp	0.1962
Ki	21.6000
<b>Inverter</b>	
Vdc	500V
Switching frequency	5KHz

Figure 10 shows the evolution of the wind for an average value of 10.5ms which will subsequently be considered as an input quantity of the turbine.

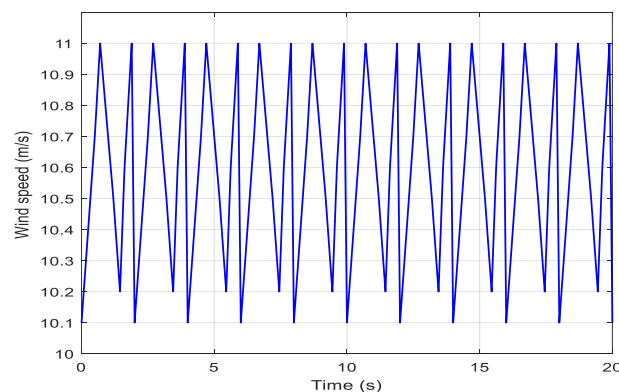


Figure 10 Wind speed

The simulation of the indirect power control of the DFIG at 0.5 MW, was implemented under MATLAB/Simulink, imposing the reference of reactive powers at zero, while the DFIG is controlled at variable speed, According to Figure 11,, the stator power reactive set point will be kept zero ( $Q_s\text{-ref} = 0\text{MVAR}$ ), this is the objective of the next test.

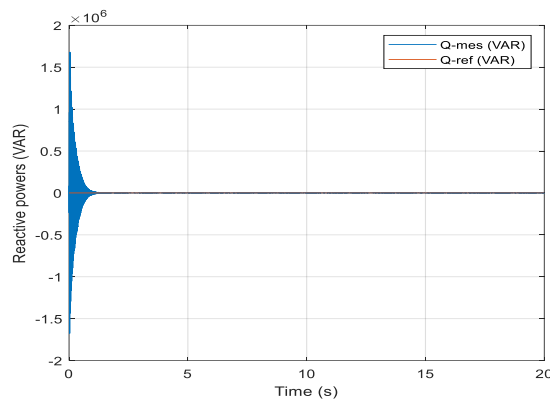


Figure 11 Reactive powers and its reference connected to the grid

Figure 12 illustrates the active power injected into the array by the assembly. We set ourselves a zero instru, We can conclude that, under the proposed control algorithm, the grid power amounts track their references values with smooth profiles. Also, from these figures, it can be noticed, that only the active power generated by the proposed system is fully delivered to the AC grid, while the reactive power is controlled to be zero. Figure 12 illustrates the reactive power injected into the array by the assembly. We set ourselves a zero instruction to have a unity power factor on the network side.

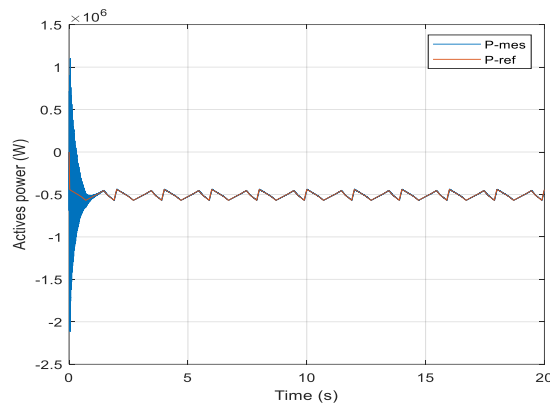


Figure 12 Active powers and its reference connected to the grid

Figures 13 represent the stator voltage connected to the grid.

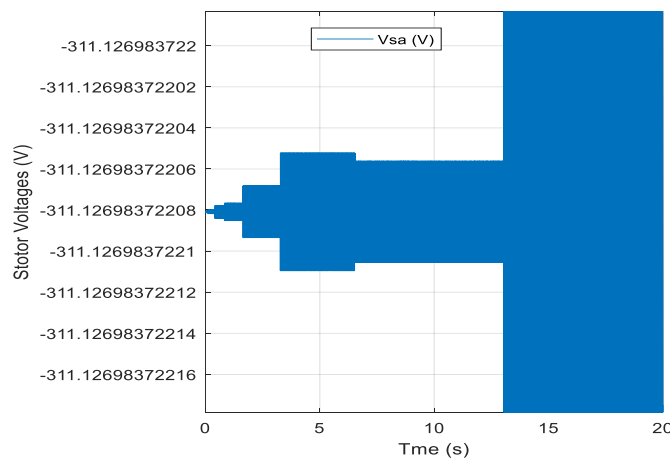


Figure 13 Stator Voltage connected to the grid

The stator current generated by the DFIG which has a sinusoidal shape (Figure 14 and Figure 15), which means a good quality of energy supply to the power grid.

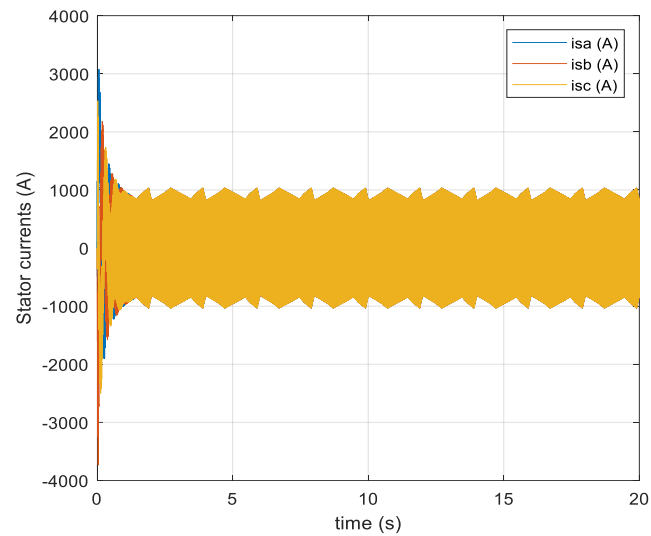


Figure 14 Stator currents

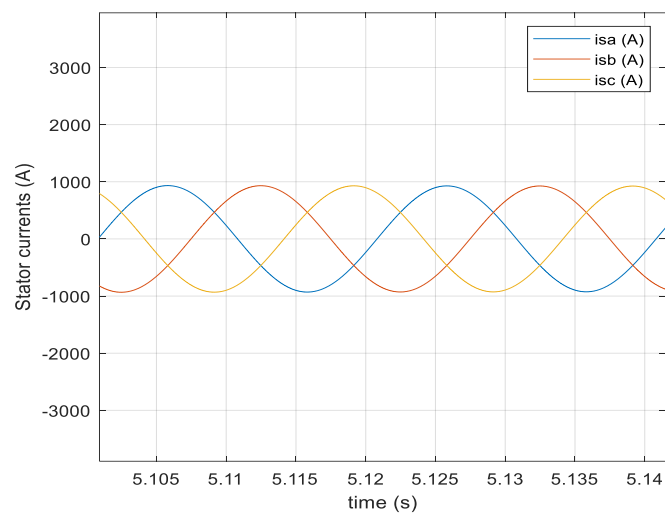


Figure 15 Zoom of Stator currents

Figure 16 shows the spectra harmonics of a phase of the stator current, it can be seen that both methods give a result satisfactory and a good THD = 0.47%. Which that explains the improvement in quality currents injected into the grid by the reduction of harmonics distortion.

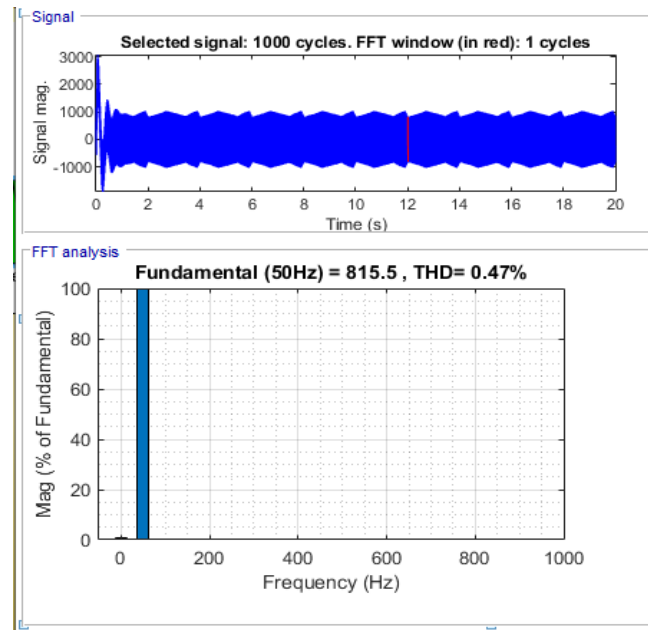


Figure 16 Spectra harmonics of stator current

#### 4. Conclusion

In this paper, wind conversion system based on doubly fed induction generator connected to the grid has been presented. In order to control the active and reactive power injected to the grid, a strategy control based on indirect power control using PWM technique with PI controller have been explored. The simulation results are satisfactory, have a good performances static and dynamic and good control proprieties between measured and reference quantities. The results encourage a further development of this study to obtain clean energy.

#### REFERENCES

- [1] Y. Liu, T. Yang, W. Teng and X. Sun, "Day-Ahead Energy Power Forecasting under Carbon Neutrality Based on XGBoost," 2023 8th Asia Conference on Power and Electrical Engineering (ACPEE), Tianjin, China, 2023, pp. 2044-2053, doi: 10.1109/ACPEE56931.2023.10135855.
- [2] Y. A. Medvedkina and A. V. Khodochenko, "Renewable Energy and Their Impact on Environmental Pollution in the Context of Globalization," 2020 International Multi-Conference on Industrial Engineering and Modern Technologies (FarEastCon), Vladivostok, Russia, 2020, pp. 1-4, doi: 10.1109/FarEastCon50210.2020.9271508.
- [3] A. Hassan, A. U. Rehman, N. Shabbir, S. R. Hassan, M. T. Sadiq and J. Arshad, "Impact of Inertial Response for the Variable Speed Wind Turbine," 2019 International Conference on Engineering and Emerging Technologies (ICEET), Lahore, Pakistan, 2019, pp. 1-6, doi: 10.1109/CEET1.2019.8711826.
- [4] A.G. Olabi, K. Obaideen, M.A. Abdelkareem, M.N. AlMallahi, N. Shehata, A.H. Alami, A. Mdallal, A.A.M. Hassan, E.T. Sayed, Wind Energy Contribution to the Sustainable Development Goals: Case Study on London Array. Sustainability 2023, 15, 4641. <https://doi.org/10.3390/su15054641>
- [5] S. Rajendran, D. Jena and M. Diaz, "Complementary Terminal Sliding Mode Control for Variable Speed Wind Turbine," 2023 International Conference on Power, Instrumentation,

- Control and Computing (PICC)*, Thrissur, India, 2023, pp. 1-5, doi: 10.1109/PICC57976.2023.10142452.
- [6] D. S. Zinger and E. Muljadi, "Annualized wind energy improvement using variable speeds," in *IEEE Transactions on Industry Applications*, vol. 33, no. 6, pp. 1444-1447, Nov.-Dec. 1997, doi: 10.1109/28.649954.
- [7] K. E. Johnson, L. Y. Pao, M. J. Balas and L. J. Fingersh, "Control of variable-speed wind turbines: standard and adaptive techniques for maximizing energy capture," in *IEEE Control Systems Magazine*, vol. 26, no. 3, pp. 70-81, June 2006, doi: 10.1109/MCS.2006.1636311.
- [8] X. Zhang, S. Qin, S. Li and C. Qi, "Modeling and Dynamic Performance Analysis of Grid Forming Doubly-fed Wind Turbine," *2023 IEEE 6th International Electrical and Energy Conference (CIEEC)*, Hefei, China, 2023, pp. 1084-1089, doi: 10.1109/CIEEC58067.2023.10166502.
- [9] G. Ofualagba and E. U. Ubeku, "Wind energy conversion system- wind turbine modeling," 2008 IEEE Power and Energy Society General Meeting - Conversion and Delivery of Electrical Energy in the 21st Century, Pittsburgh, PA, USA, 2008, pp. 1-8, doi: 10.1109/PES.2008.4596699.
- [10] A. B. Cultura and Z. M. Salameh, "Modeling and simulation of a wind turbine-generator system," *2011 IEEE Power and Energy Society General Meeting*, Detroit, MI, USA, 2011, pp. 1-7, doi: 10.1109/PES.2011.6039668.
- [11] M. L. Corradini, G. Ippoliti and G. Orlando, "Robust Control of Variable-Speed Wind Turbines Based on an Aerodynamic Torque Observer," in *IEEE Transactions on Control Systems Technology*, vol. 21, no. 4, pp. 1199-1206, July 2013, doi: 10.1109/TCST.2013.2257777.
- [12] N. W. Miller, J. J. Sanchez-Gasca, W. W. Price and R. W. Delmerico, "Dynamic modeling of GE 1.5 and 3.6 MW wind turbine-generators for stability simulations," *2003 IEEE Power Engineering Society General Meeting (IEEE Cat. No.03CH37491)*, Toronto, ON, Canada, 2003, pp. 1977-1983 Vol. 3, doi: 10.1109/PES.2003.1267470.
- [13] A. Henry, M. Pusch and L. Pao, "Modeling Blade-Pitch Actuation Power Use in Wind Turbines," *2023 American Control Conference (ACC)*, San Diego, CA, USA, 2023, pp. 1480-1485, doi: 10.23919/ACC55779.2023.10156073.
- [14] M. Marinelli, A. Morini, A. Pitto and F. Silvestro, "Modeling of doubly fed induction generator (DFIG) equipped wind turbine for dynamic studies," *2008 43rd International Universities Power Engineering Conference*, Padua, Italy, 2008, pp. 1-6, doi: 10.1109/UPEC.2008.4651589.
- [15] J. B. Ekanayake, L. Holdsworth, XueGuang Wu and N. Jenkins, "Dynamic modeling of doubly fed induction generator wind turbines," in *IEEE Transactions on Power Systems*, vol. 18, no. 2, pp. 803-809, May 2003, doi: 10.1109/TPWRS.2003.811178.
- [16] P. Osekar, S. Kalligudd, S. Angadi and A. B. Raju, "Field Oriented Control of Surface-mount PMSM using Model Predictive Current Control," *2022 IEEE North Karnataka Subsection Flagship International Conference (NKCon)*, Vijaypur, India, 2022, pp. 1-5, doi: 10.1109/NKCon56289.2022.10126799.
- [17] D. Zellouma, H. Benbouhenni, N. Bizon and Y. Bekakra, "A New Field-Oriented Control for Induction Motor Drive Using a Synergetic-Super Twisting Algorithm," *2023 15th*

- International Conference on Electronics, Computers and Artificial Intelligence (ECAI), Bucharest, Romania, 2023, pp. 1-6, doi: 10.1109/ECAI58194.2023.10193989.
- [18] F. Yusivar, N. Hidayat, R. Gunawan and A. Halim, "Implementation of field oriented control for permanent magnet synchronous motor," 2014 International Conference on Electrical Engineering and Computer Science (ICEECS), Kuta, Bali, Indonesia, 2014, pp. 359-362, doi: 10.1109/ICEECS.2014.7045278.
- [19] N. J. Antony, D. Mishra and S. Parveen, "Sensorless Field Oriented Control of AC Induction Motor Using PI, PD & PID Controllers," 2022 IEEE North Karnataka Subsection Flagship International Conference (NKCon), Vijaypur, India, 2022, pp. 1-5, doi: 10.1109/NKCon56289.2022.10126557.
- [20] K. Rahman et al., "Field-Oriented Control of Five-Phase Induction Motor Fed From Space Vector Modulated Matrix Converter," in IEEE Access, vol. 10, pp. 17996-18007, 2022, doi: 10.1109/ACCESS.2022.3142014.
- [21] H. Gasmi, H. Benbouhenni, N. Bizon and S. Mendaci, "Field-Oriented Control Based on Nonlinear Techniques for Wind Energy Conversion Systems," 2023 15th International Conference on Electronics, Computers and Artificial Intelligence (ECAI), Bucharest, Romania, 2023, pp. 1-7, doi: 10.1109/ECAI58194.2023.10194068.
- [22] F. Blaschke, « A new method for the structural decoupling of A.C. induction machines »; In Conf. Rec. IFAC, Dussesrdorf, Germany, Oct.1971.
- [23] H. Lhachimi, Y. Sayouti and Y. Elkouari, "Direct power control of a DFIG fed by a two level inverter using SVM algorithm," 2017 International Conference on Modern Electrical and Energy Systems (MEES), Kremenchuk, Ukraine, 2017, pp. 12-15, doi: 10.1109/MEES.2017.8248866.
- [24] S. Gao, H. Zhao, Y. Gui, D. Zhou, V. Terzija and F. Blaabjerg, "A Novel Direct Power Control for DFIG With Parallel Compensator Under Unbalanced Grid Condition," in IEEE Transactions on Industrial Electronics, vol. 68, no. 10, pp. 9607-9618, Oct. 2021, doi: 10.1109/TIE.2020.3022495.
- [25] Trivedi et al.: A Review on Direct Power Control for Applications to Grid Connected PWM Converters, Engineering, Technology & Applied Science Research Vol. 5, No. 4, 2015, 841-849
- [26] M. Mohamed, H. Wang and Y. Tiang, "Indirect power control of DFIG based wind turbine using fractional order intelligent proportional integral sliding mode controller," 2021 40th Chinese Control Conference (CCC), Shanghai, China, 2021, pp. 5939-5944, doi: 10.23919/CCC52363.2021.9549563.
- [27] A. Olloqui *et al.*, "Indirect power control of a DFIG using model-based predictive rotor current control with an indirect matrix converter," 2015 IEEE International Conference on Industrial Technology (ICIT), Seville, Spain, 2015, pp. 2275-2280, doi: 10.1109/ICIT.2015.7125433.
- [28] Y. Ihedrane, C. El Bekkali and B. Bossoufi, "Direct and indirect field oriented control of DFIG-generators for wind turbines variable-speed," 2017 14th International Multi-Conference on Systems, Signals & Devices (SSD), Marrakech, Morocco, 2017, pp. 27-32, doi: 10.1109/SSD.2017.8166915.
- [29] R. R. Patra and A. Banerjee, "Indirect Vector Control of DFIG Based Wind Energy System Using Fuzzy-PI Controller," 2018 2nd International Conference on Power, Energy and

- Environment: Towards Smart Technology (ICEPE)*, Shillong, India, 2018, pp. 1-6, doi: 10.1109/EPETSG.2018.8659135.
- [30] I. Zgarni and L. El Amraoui, "Dynamic Modeling and Vector control of DFIG-based Wind Turbine," *2022 5th International Conference on Advanced Systems and Emergent Technologies (IC\_ASET)*, Hammamet, Tunisia, 2022, pp. 262-267, doi: 10.1109/IC\_ASET53395.2022.9765917.
- [31] C. Du, X. Du, C. Tong, Y. Li and P. Zhou, "Stability Analysis for DFIG-Based Wind Farm Grid-Connected System Under All Wind Speed Conditions," in *IEEE Transactions on Industry Applications*, vol. 59, no. 2, pp. 2430-2445, March-April 2023, doi: 10.1109/TIA.2022.3218022.
- [32] S. Ghosh, "Closed loop control of a DFIG based wind power system," *2013 IEEE Innovative Smart Grid Technologies-Asia (ISGT Asia)*, Bangalore, India, 2013, pp. 1-6, doi: 10.1109/ISGT-Asia.2013.6698738.
- [33] H. M. Moghadam, M. Gheisarnejad, Z. Esfahani and M. -H. Khooban, "A Novel Supervised Control Strategy for Interconnected DFIG-Based Wind Turbine Systems: MiL Validations," in *IEEE Transactions on Emerging Topics in Computational Intelligence*, vol. 5, no. 6, pp. 962-971, Dec. 2021, doi: 10.1109/TETCI.2020.3010060.
- [34] S. Liu, Y. Han, C. Du, S. Li and H. Zhang, "Fuzzy PI Control for Grid-side Converter of DFIG-based Wind Turbine System," *2021 40th Chinese Control Conference (CCC)*, Shanghai, China, 2021, pp. 5788-5793, doi: 10.23919/CCC52363.2021.9550601.
- [35] O. Al Zabin and A. Ismael, "Rotor Current Control Design for DFIG-based Wind Turbine Using PI, FLC and Fuzzy PI Controllers," *2019 International Conference on Electrical and Computing Technologies and Applications (ICECTA)*, Ras Al Khaimah, United Arab Emirates, 2019, pp. 1-6, doi: 10.1109/ICECTA48151.2019.8959530.
- [36] O. P. Bharti, R. K. Saket and S. K. Nagar, "Design of PI controller for doubly fed induction generator using static output feedback," *2015 39th National Systems Conference (NSC)*, Greater Noida, India, 2015, pp. 1-6, doi: 10.1109/NATSYS.2015.7489128.
- [37] D. Izci, S. Ekinici, C. Budak and V. Gider, "PID Controller Design for DFIG-based Wind Turbine via Reptile Search Algorithm," *2022 Global Energy Conference (GEC)*, Batman, Turkey, 2022, pp. 154-158, doi: 10.1109/GEC55014.2022.9986617.
- [38] C. Z. El Archi, T. Nasser, A. Essadki and J. Alvarado, "Real Power Control: MPPT and Pitch Control in a DFIG Based Wind Turbine," *2020 3rd International Conference on Advanced Communication Technologies and Networking (CommNet)*, Marrakech, Morocco, 2020, pp. 1-6, doi: 10.1109/CommNet49926.2020.9199625.